# The interaction between curvature and lateral shear vorticities in a mean and an instantaneous Florida Current, a comparison

By FRANK CHEW, *Atlantic Oceanographic and Meteorological Labs., Environmental Research Laboratories, NOAA, Miami, Florida 33149, USA*

(Manuscript received March 12, 1974; in final form Jan. 9, 1975)

ABSTRACT

The question of how much of the dynamics of an instantaneous current is retained in the dynamics of a model derived from its mean structure is considered in terms of a comparison between two case studies of the Florida Current. In the mean model, fluid elements are restrained from crossing the speed axis. But in an observation of an instantaneous current there was an interaction between curvature and lateral shear vorticities accompanied by a systematic movement of fluid elements across the speed axis. This difference is considered from two points of view. The first is that of the equations governing the interaction process, particularly the banking mechanism that converts curvature vorticity to lateral shear vorticity and vice versa. The second is that of the dynamics of the geostrophic potential vorticity. It is concluded that, because of the imposed geostrophic constraint, the mean model does not retain the interaction process.

## Introduction

The most concise statement of the dynamics of an adiabatic, inviscid flow is the law of conservation of potential vorticity. However, for diagnostic studies the relative vorticity equation is more useful because it brings out the mechanisms that change the relative vorticity. In this sense, the curvature and lateral shear vorticity equations derived by Chew (1974) are even more useful because they bring out the mechanisms that govern the individual change of curvature and lateral shear vorticities separately. One of these mechanisms induces interaction between the curvature and lateral shear vorticity. The purpose of this paper is to detail a manifestation of the interaction and to compare the manifestation in two studies of the Florida Current. One is the model of a mean current constructed by Schmitz (1969), and the other is an instantaneous current observed by Chew (1974).

In the special case of a fluid element situated initially in the instantaneous speed axis of a meandering current at the point of inflection, the process of interaction takes on a unique form. An observer riding with the element will find the speed axis of the current alternately forming to his left and right depending on the sign of the flow curvature. Equivalently, an observer using the changing location of the speed axis as a reference will find the fluid element moving across the speed axis. This crossing of the axis is related to a characteristic cross-stream distribution of potential vorticity. Hence the comparison of the interaction process may be phrased in terms of potential vorticity conservation. But the mere satisfaction of the conservation law does not imply an identity or even a similarity in dynamics. For the law applies equally, e.g., to both linear and non-linear regimes. Our consideration of the interaction process in the context of the conservation law will serve also to illustrate this point.

The mean model constructed by Schmitz was based on data collected over a 30-day period in 1965 in a segment of the Florida Current downstream of the segment observed by Chew in a 5-day period in 1971. These differences in time and place are assumed immaterial on the premise that the dynamics of the Florida Current remained unchanged.

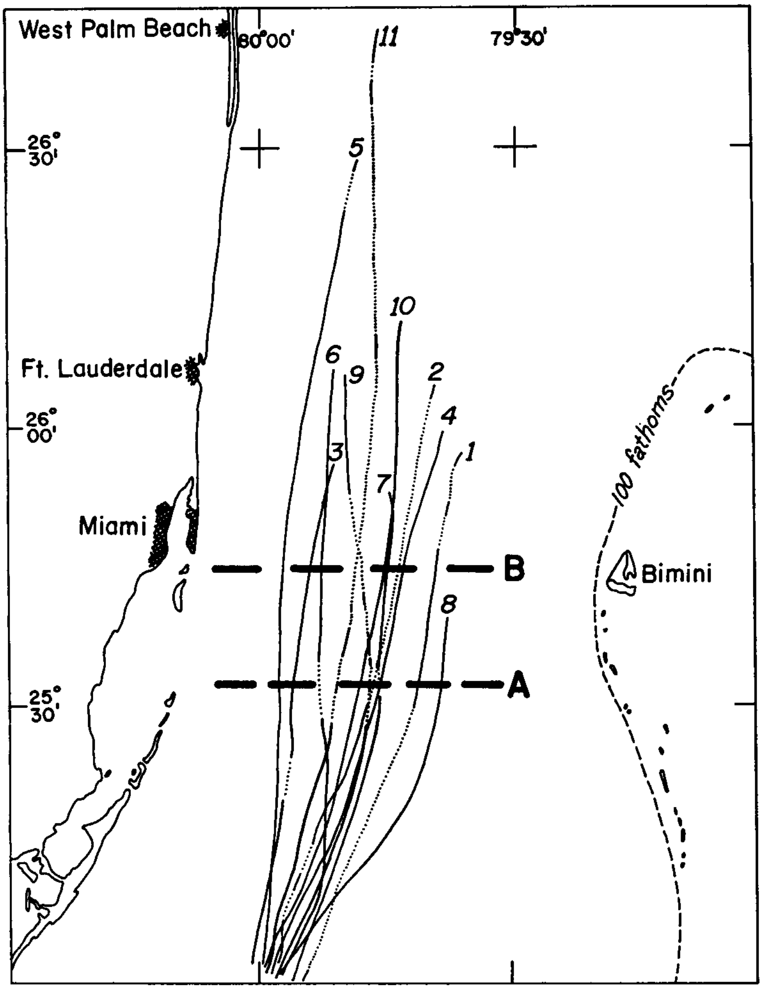


*Fig. 1.* The two dashed lines $A$ and $B$ mark the locations of velocity and density observations made by Schmitz in the period 24 May to 24 June, 1965. The curvilinear lines 1 to 11 mark the paths of shallow drifting drogues made by Chew & Berberian in the period 15 February to 9 March, 1969.

First the model of the mean current is summarized and the features of interest identified. Next, comparable features for the instantaneous current and their interpretation from the viewpoint of potential vorticity conservation are presented. To explain the dynamics involved, the formulation of the equations that govern the individual change of curvature and lateral shear vorticities separately are next reviewed. Finally, by use of these equations the limitations of the dynamics of the mean model are shown.

## Potential vorticity in a mean Florida Current

From a series of velocity and density measurements taken along the two lines labelled $A$ and $B$ in Fig. 1, Schmitz constructed a model of a mean Florida Current in terms of a single moving layer whose thickness, $H$, he identified as equal to the thickness of the surface layer with a vertically averaged sigma-$t$ of 25.0. Fig. 2 shows his cross-stream distribution of the thickness of the layer and its corresponding

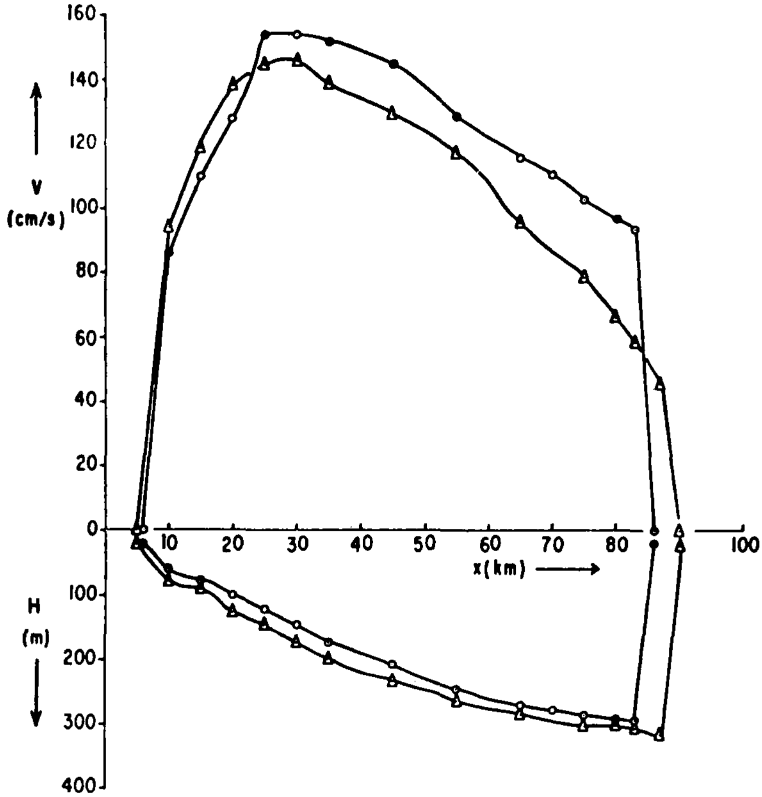


*Fig. 2.* Downstream speed ($v$) and layer depth ($H$) vs. cross-stream distance ($x$). Triangles for section $A$ and circles for section $B$ as shown in Fig. 1. Reproduced from Schmitz (1969).

downstream speed. The feature of direct interest is the locations of the speed axes between 25 and 30 km.

For the one-moving-layer model, the potential vorticity of an individual column is the ratio of its absolute vorticity to its thickness, $H$. The absolute vorticity is a sum of the vertical components of the planetary and relative vorticities. Because his data did not permit an adequate evaluation of the significance of the curvature vorticity, Schmitz made the assumption of equating the relative vorticity to the lateral shear vorticity alone. Using this assumption and the distribution of variables in Fig. 2, Schmitz computed the potential vorticity at different locations along the two lines to obtain the cross-stream distributions shown in Fig. 3, whose principal feature is that east of km 30, the distributions of potential vorticity are relatively uniform, but that to the west of km 30, in the regions of both the speed axes and the left flanks the distributions show a steep rise in potential vorticity. In a regime where potential vorticity is conserved, fluid elements with a given potential vorticity may move only to regions where the potential vorticity is the same. In the right flank east of km 30 in Fig. 3, if the small cross-stream variation in potential vorticity may be ignored, individual columns there can move laterally without constraint. However, in the regions of both the speed axis and the left flank, because of the large change in potential vorticity, individual columns in these regions are constrained to remain in their relative lateral positions. In consequence, there can be no flow across the speed axis. The comparison centers on the determination of whether or not this consequence holds also for an instantaneous Florida Current. The direct way to find out is to observe the lateral movements of individual parcels relative to the instantaneous speed axis.

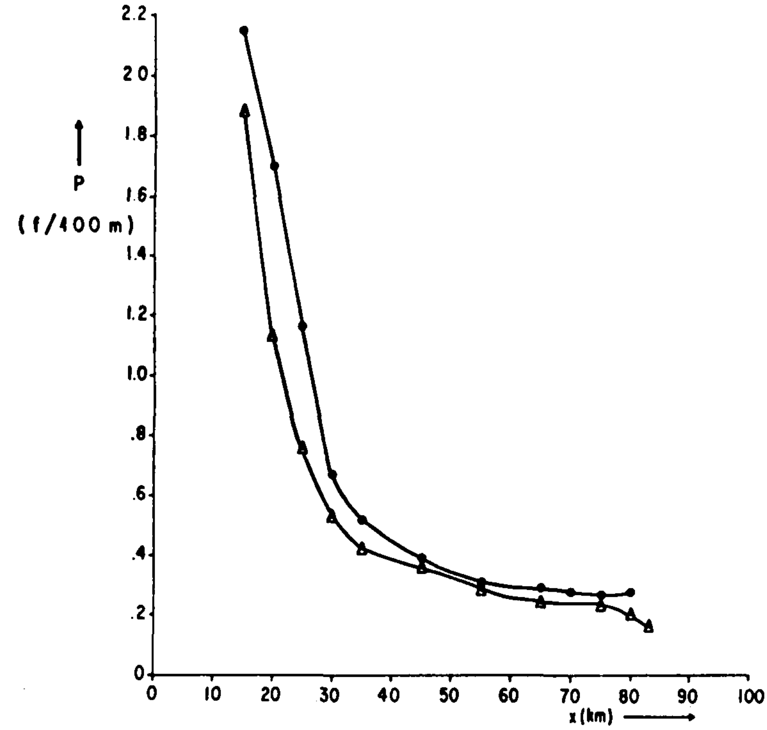


*Fig. 3.* Potential vorticity ($P$) vs. cross-stream distance ($x$). Triangles for section $A$ and circles for section $B$ as shown in Fig. 1. Reproduced from Schmitz (1969).

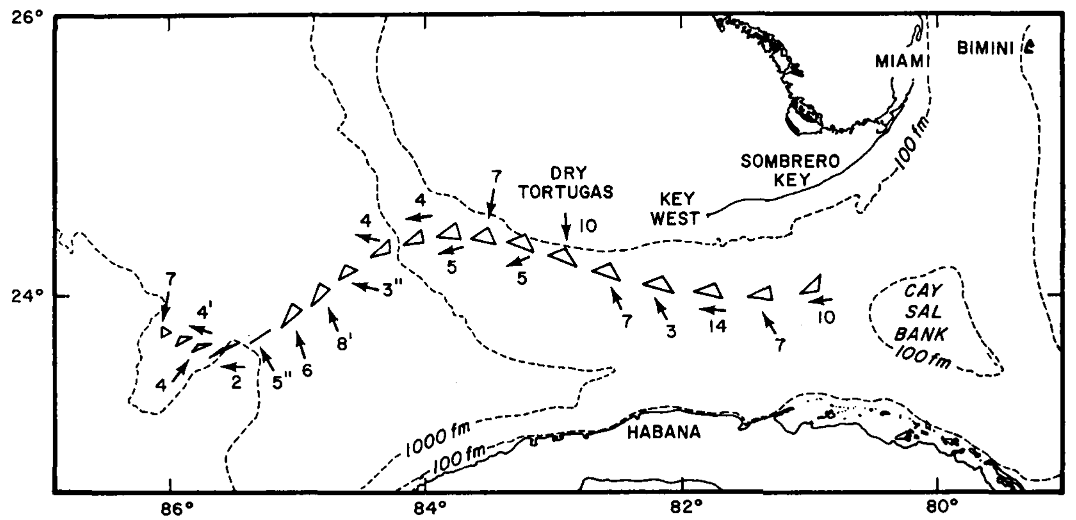


*Fig. 4.* Path of drogue formation and encountered winds in the observation of 1971. Individual drogues located at the vertices of the triangles spaced six hours apart. The time for the first triangle is 0000 hr (Universal Time), August 27. Arrows represent directions of winds as observed from the drogue-tracking ship, and numerals give wind strengths in knots, both corrected for ship drift. The time of each plotted wind corresponds to the time of the nearest plotted drogue formation, with the exception of four cases indicated by numerals with prime and double primes. The single prime cases are off the indicated time by one hour, the double primes cases two hours.

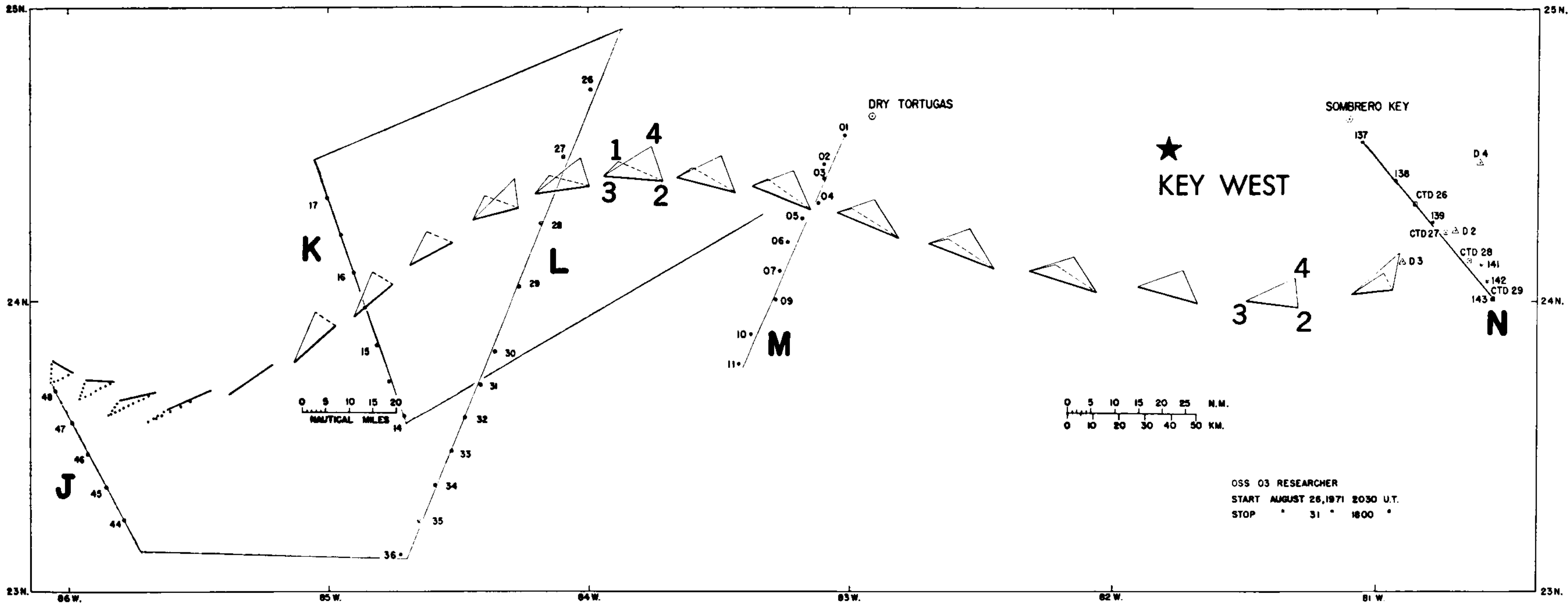


*Fig. 5.* Drogue positions at vertices of triangles spaced six hours apart. The first drogue was deployed at 2030 hr (U.T.) on August 26 1971, but the first drogue formation shown on the extreme left corresponds to 0000 hr (U.T.) the next day. One drogue was re-deployed on the second day. Drogues 2 and 3 drifted freely throughout the 5-day observation. Drogue 4 was added on the third day. Reproduced from Chew (1974).

However, we anticipate that measurement uncertainty and interference of other processes will render the observation imprecise, and that in conjunction with observation it is necessary as well to consider the general interaction process of which the crossing of the speed axis is but one manifestation. The observation is presented first.

## Observation of an instantaneous Florida Current

Figs. 4 and 5 summarize Chew's observation of the Florida Current by means of free-drifting drogues at a 40 m depth. Three drogues were initially deployed 200 km north of the Yucatan Strait as shown in Fig. 4, whose salient feature is the lack of significant downstream reduction in the meandering amplitude of the current in spite of large decreases in both the water depth and channel width. Shown in Fig. 5 for every six hours, are the drogue formations obtained by connecting simultaneous drogue positions with straight lines. Because all drogues presumably drifted at a constant depth, and because parcel motion is three-dimensional even in large-scale flow, the drogue formation did not track the same parcel throughout. But if the vertical advection is only a small part of the individual change, then the individual change is approximated well by the change in drogue formation. This is assumed; and in this context we shall refer to the tracking of a single parcel. The justification will be given later after the appropriate equations are presented. Moreover, the sign of the path curvature was observed, but according to Blaton's equation the observation also gives the sign of the stream-line curvature provided the current is quasi-steady. This is also assumed. In the reference frame of natural coordinates, with positive cross-stream direction to the left, the lateral shear is negative when, in a drogue formation, the drogues on the left lagged behind the drogues on the right; and the lateral shear is positive when the drogues on the right lagged behind the drogues on the left. Accordingly, in Fig. 5 where the curvatures were positive at the two cyclonic bends, the lateral shears were also positive, and where the curvature was negative at the anticyclonic bend the shear was also negative.[1] Because these different sign combinations are those of an individual parcel tracked by the drogue formation, the curvature and lateral shear of the parcel must turn zero somewhere between, say, the positive curvature and lateral shear at the cyclonic bend and the negative curvature and lateral shear at the downstream anticyclonic bend. Moreover, it is plausible that the curvature and the lateral shear both turned zero together. In Fig. 5 at the two inflection points near sections $K$ and $M$ where the curvatures were zero, the lack of significant change in the shape of the two successive six-hour drogue formations there indicates that the accompanying lateral shears were also zero. Hence the relationship is one of the sign of the lateral shear following the sign of the flow curvature.

Now, for simplicity, consider a meandering current with a single speed axis, a situation quite consistent with the temperature sections shown in Fig. 6 where cross-stream isothermal slopes are generally largest in the water columns supporting the drogue formations. In this case, negative lateral shear is confined to the left flank, and positive shear to the right flank. It follows that a drogue formation is in the speed axis when the shear is zero, in the left flank when the shear is negative, and in the right flank when the shear is positive. Accordingly, in following the movement of the parcel downstream from the inflection near section $K$ in Fig. 5, we see that the parcel moved off the speed axis and entered the left flank on approaching the anticyclonic turn. Then on moving out of the anticyclonic turn, the parcel also moved laterally out of the left flank and re-entered the speed axis as the curvature of the path became zero at the inflection point downstream of section $M$. Finally, on approaching the cyclonic turn, the parcel again moved laterally off the speed axis, but this time into the right flank. Thus the parcel elements crossed the speed axis systematically. This is in sharp disagreement with the requirement contained in the model presented by Schmitz. Before explaining the disagreement, attention will be given first to the likely effects of local winds on the drift of the drogues and of the

[1] In Fig. 20 in the paper by Chew (1974) the speed differences at the anticyclonic bend show a positive shear. This is discounted here, because errors in speed estimates are 10 cm/s, and there is also the possible presence of a local interfering phenomenon.

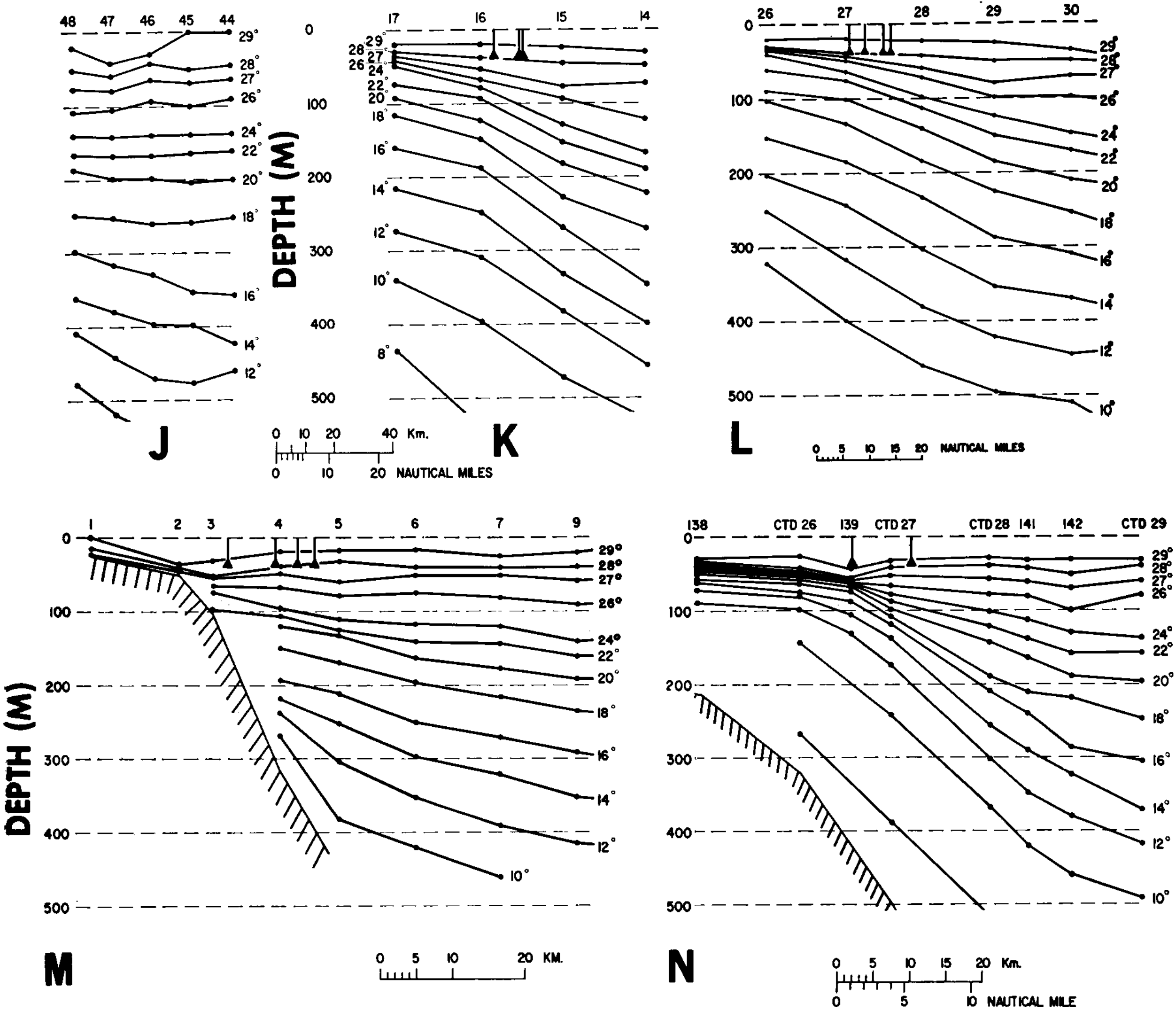


*Fig. 6.* Temperature distribution along sections *J*, *K*, *L*, *M* and *N* shown in Fig. 5. Adapted from Chew (1974).

downstream channel constriction off Miami on the interaction between curvature and lateral shear there.

## Wind effect and channel constriction

Some of the local winds observed from the drogue-tracking ship while drifting with the current are shown in Fig. 4. The winds encountered were generally light. So light that in a direct test of wind effect on drogue systems with different surface buoys, Chew (1974) found these winds to have essentially the same effects even though the sail areas of the buoys were much different. Strong and persistent winds can be an important source of error, but a typical wind strength in Fig. 4 is only 7 knots. According to a diagram given by Brown (1959), the approximate effect of a 7-knot wind is to drag the drogue system through the water at 1.7 cm/s. This is small compared with the speed of the current. Moreover, since the wind directions were variable and bear no apparent relationship to the large systematic lateral movement of the drogues, the winds encountered may be dismissed as a significant factor in the observed interaction.

As shown in Fig. 1, there is a channel constriction in the region where Schmitz constructed his mean model. The question is, does the constriction effectively suppress the interaction between curvature and lateral shear, and hence the crossing of the speed axis? There is reproduced in Fig. 1 from the work of Chew & Berberian (1972), the mean paths of eleven lines of three drogues each. The lines, all starting from a common area, were each tracked for about one day in the order in which they are numbered in the figure. As successive lines were tracked, the curvatures took on different signs and magnitudes as in the passage of a meander train. Detailed in the original work, but not reproduced here, are the lateral shears accompanying the flow curvatures. But primarily because these lines are short, the sign of the flow curvature is sometimes in doubt. But where the curvature sign is clear cut, as for lines 5, 8, 10, and 11 in Fig. 1, the sign of the shear clearly follows the sign of the curvature. This agreement in signs suggests the probability that had each line been tracked for a longer period, the interaction between curvature and shear in general, and the crossing of the speed axis in particular would have been more clearly delineated. Hence it is concluded that it is not the channel constriction, but an artifact of the mean model that suppressed the interaction. To understand the artifact, it is necessary first to understand the mechanism responsible for the interaction. And to emphasize the relation of the interaction to the general process that maintains the conservation of potential vorticity, we consider first a condition imposed by the conservation.

## An imposed condition

In a natural coordinate system with geometric height as vertical axis, let the components of a three-dimensional velocity be written $\mathbf{V} = V\mathbf{s}$ for the horizontal, and $w\mathbf{k}$ for the upward component; $\mathbf{n} = \mathbf{k} \times \mathbf{s}$ is positive to the left of $\mathbf{V}$. Hence in natural coordinates $(s, n, z, t)$, the vertical component of relative vorticity, $\zeta$, is given by

$$\zeta = K_s V - (\partial V/\partial n) \tag{1}$$

where $K_s$ is the streamline curvature. In (1) the definition of lateral shear vorticity includes the negative sign; e.g., a flow with slower current to the left represents negative lateral shear but positive lateral shear vorticity. Then, with the usual assumption, the law of conservation of potential vorticity in the ocean may be written

$$(f + \zeta)/h' = \text{constant} \tag{2}$$

where $h'$ is the vertical thickness of a parcel element. When the constant is evaluated at a streamline inflection where values are denoted by the subscript "0", and use is made of eq. (1), eq. (2) may be expanded to give

$$\partial V/\partial n = K_s V + (f - f_0 h'/h_0') + (\partial V/\partial n)_0 (h'/h_0') \tag{3}$$

Hence for parcel elements initially in the speed axis at an inflection of a meandering current, eq. (3) reduces to

$$\partial V/\partial n = K_s V + (f - f_0 h'/h_0') \tag{4}$$

Therefore, in order that the sign of the lateral shear of the parcel follows the sign of its flow curvature, it is necessary and sufficient for the curvature term in (4) to have a magnitude larger than the Coriolis term. This condition may be rephrased. From eqs. (1) and (4) the term inside the parentheses is seen equal to the negative of the relative vorticity,

$$(f - f_0 h'/h_0') = -\zeta \tag{5}$$

Consequently, the condition is equivalent to the following inequality in absolute magnitudes,

$$|K_s V| > |\zeta| = |K_s V - \partial V/\partial n| \neq 0 \tag{6}$$

where $\zeta = 0$ is excluded, for reasons that will be given later. Accordingly, in addition to the requirement of a sign difference between the curvature and lateral shear vorticities, the inequality (6) will hold when the absolute magnitudes of the individual change of the two vorticities are given by

$$|(D/Dt)(K_s V)| > |(D/Dt)(-\partial V/\partial n)| \tag{7}$$

Thus for a flow where potential vorticity is conserved, and for a parcel initially located in the speed axis at an inflection of the flow, the conditions (6) and (7) must be met, if the sign of the lateral shear is to follow the sign of the flow curvature. The two derivatives in (7) have been discussed by Chew (1974). These are first reviewed, starting off with the equation governing the individual change of curvature or turning vorticity, called the turning equation.

## The turning equation

The turning equation, whose derivation is detailed by Chew (1974), is

$$(D/Dt)\,K_s V = \underbrace{(\partial/\partial n)\,(DV/Dt)}_{\text{Banking}} - \underbrace{(f+K_s V)\,\nabla\cdot\mathbf{V}}_{\text{Divergence}} - \underbrace{K_s V(\partial V/\partial s)}_{\text{Curvature}} - \underbrace{Df/Dt}_{\text{Beta}} \qquad (8)$$

The individual change of the turning vorticity is a function of four terms: the beta term; a curvature-acceleration term, a product of the curvature and the downstream acceleration; a divergence term, similar to the corresponding term in the relative vorticity equation but without the shear vorticity; and the banking term that involves the cross-stream change of the downstream acceleration, hence of the downstream pressure gradient force, and thus represents a pressure torque.

The banking mechanism has both barotropic and baroclinic components. The first is derived from changes in the height of the sea surface, and the second from changes in the subsurface density field. For steady state motion, the barotropic component of the banking term may be written,

$$(\partial/\partial n)(DV/Dt)_h = -(g/V)_h(\partial w/\partial n)_h + g(w/V^2)_h(\partial V/\partial n)_h \qquad (9)$$

where all the terms are evaluated at the sea surface, $h$. Thus the barotropic component of the banking mechanism is negative when, e.g., the sea surface, especially one with negative lateral shear, rises faster on the left than on the right. A differential raising of the sea surface across the stream will pile up mass to the sides at different rates. This will tend to turn the speed axis of the current away from the side where the sea surface is rising faster, simply because that side of the current is losing kinetic energy more rapidly.

The nature of the baroclinic component of the banking mechanism in a steady flow may be seen from the downstream component of the equation of frictionless motion for a parcel at a subsurface height, $z$, in the form:

$$DV/Dt = (g/\varrho)\int_z^h (w/V)\,(\partial\varrho/\partial z)\,dz - g(w/V)_h \qquad (10)$$

where the integration extends to the sea surface, $h$. As only stable stratification is considered, the sign of the baroclinic term in (10) is determined by the sign of the vertical motion. In general, the sign of the vertical motion in a water column may change with height, but in the height interval $(h–z)$ where the sign is the same, parcel decelerates when ascending and accelerates when descending. Hence vertical motion plays a central role in the banking mechanism, which also affects the lateral shear vorticity, as we see next.

## The lateral shear equation

The procedure used in deriving the turning eq. (8) also gives the equation governing the individual change of lateral shear vorticity,

$$(D/Dt)\,(-\partial V/\partial n) = \underbrace{-\partial/\partial n)\,(DV/Dt)}_{\text{Banking}} + \underbrace{(\partial V/\partial n)\,\nabla\cdot\mathbf{V}}_{\text{Divergence}} + \underbrace{K_s V(\partial V/\partial s)}_{\text{Curvature}} + \underbrace{(\partial w/\partial n)\,(\partial V/\partial z)}_{\text{Twisting}} \qquad (11)$$

In this equation the important feature is the presence of both the banking and curvature terms but with signs opposite to their counterparts in the turning eq. (8); therefore they serve to transform curvature vorticity to lateral shear vorticity and vice versa. But since lateral shear is the negative of lateral shear vorticity, the presence of the banking and curvature-acceleration mechanisms in both (8) and (11) ensures the simultaneous generation of curvature and shear of the same sign. However, their rates of generation will be different.

## The rate of curvature and shear vorticities changes

The operation $(D/Dt)$, representing the individual change following the three-dimensional motion of a parcel, may be decomposed into a horizontal time change $(d/dt)$, and a vertical advection. That is, $D/Dt = d/dt + w(\partial/\partial z)$. In cases where there is conservation following the parcel, the vertical advection is equal in magnitude to the horizontal time change and may not be neglected. However, this is not the case for curvature and shear vorticities changes. For the portion of the Florida Current located between sections $M$ and $N$ in Fig. 5, and except for the vertical advection term, Table 1 reproduces the estimates given by Chew (1974) of the different terms in eqs. (8) and (11). In the Table, the notation $(-1)$ (eq. 11) means a multiplication by $(-1)$ to change eq. (11) into an equation for lateral shear.

The estimate of the vertical advection listed in the Table is made as follows. East of section $M$ in Fig. 5 the drogue formation accelerated downstream. The concurrent descending motion indicated by eq. (10) for steady flow is assumed reflected in the downstream lowering of the 28C and 29C isotherms between sections $M$ and $N$ in Fig. 6. For an average lowering of 15 m over 30 hours, the descending speed was 0.015 cm/s at the level of the drogues. Then for a curvature of (1/150 km), assumed constant with height, and a vertical shear of $10^{-2}/s$, the resulting vertical advection of $K_s V$ is

$$w(\partial K_s V/\partial z) = wK_s(\partial V/\partial z) = -0.1 \times 10^{-10}/s^2 \tag{12}$$

This represents an over-estimate, since the shear, corresponding to the disappearing of a surface current of 200 cm/s at a 200 m depth, is an extreme assumption. Yet, the magnitude of (12) is still an order smaller than that of the horizontal time change.

In Table 1, the entry for vertical advection of lateral shear is assumed equal to (12). Errors for these estimates are no less than the probable errors of $\pm 46\%$ for the larger terms in Table 1. For each estimate of $K_s$ or $V$, the error is 10%, so that an estimate of, say, the curvature-acceleration term entails a compounding of errors as in a binomial expansion with exponent 4. Within these error bounds, it is possible to balance the sum of the contributions of the various terms in the Table. However, this is not done; rather, the view of large tolerance is adopted.

Table 1. *Estimates of the terms in the equations for curvature vorticity and lateral shear changes for the Florida Current*

| Term | Curvature vorticity (eq. 8) ($10^{10-}/s^2$) | Lateral shear $(-1)$ (eq. 11) ($10^{-10}/s^2$) |
|---|---|---|
| Horizontal time change | 1.2 | 1.0 |
| Vertical advection | −0.1 | −0.1 |
| Banking | 1.0 | 1.0 |
| Divergence | 1.0 | 0.2 |
| Curvature-acceleration | −0.1 | −0.1 |
| Beta effect | 0.1 | |
| Twisting | | ? |

Two conclusions may be drawn from Table 1. The first is that the horizontal time change $(d/dt)$ represents most of the individual changes in curvature and shear; hence these changes are adequately revealed by changes in a drogue formation. Second, the dominant mechanisms changing curvature vorticity are the banking and divergence mechanisms, while the banking mechanism is the only important one in lateral shear change. This difference follows directly from the absence of the Coriolis parameter in eq. (11). In curvature vorticity change, vertical motion provided the necessary link in the reinforcement observed between the banking and the divergence mechanisms. Where vertical motion is present in a shallow layer bounded on the top by the sea surface, its magnitude is least at the top so that the motion varies with height. Hence, in this layer where, e.g., descending motions accompany horizontal convergence, the pattern of descending motion that makes the banking term positive also makes the divergence term positive. Accordingly, as a parcel in the surface layer moved from its initial position in the speed axis at an inflection, the turning vorticity of the parcel changed more rapidly than its lateral shear. Thus primarily by means of the banking mechanism, both conditions (6) and (7) are fulfilled, and the observed movement across the speed axis is consistent with the constraint of potential vorticity conservation.

The sum of the turning eq. (8) and the shear vorticity eq. (11) is the relative vorticity equation which, in turn, is a differential form of the conservation eq. (2). Hence the banking and the curvature-acceleration mechanisms contained in the processes represented in (8) and (11) are implicit in the process that maintains the conservation of potential vorticity. Both ageostrophic and geostrophic mechanisms are contained in eqs. (8) and (11), and are hence implicit in the conservation eq. (2). Thus, depending on the strength of various mechanisms, the regime of potential vorticity conservation encompasses a wide variety of motion systems. A system where the sign of the lateral shear may follow the sign of the curvature is one. Another is the system of geostrophic potential vorticity.

## Geostrophic potential vorticity

In the idealization of geostrophic current where the Coriolis acceleration exactly balances the horizontal pressure gradient force, the ageostrophic components of centripetal and downstream accelerations are zero at all times. Thus in a geostrophic flow ($\mathbf{V}_g = V_g \mathbf{s}$), the eqs. (8) and (11) in ($s$, $n$, $\varrho$, $t$) coordinates reduce respectively to

$$\nabla \cdot \mathbf{V}_g = -(1/f)Df/Dt \tag{13}$$

$$\nabla \cdot \mathbf{V}_g = -(\partial V_g/\partial n)^{-1}(D/Dt)(\partial V_g/\partial n) \tag{14}$$

where all variables are evaluated along constant (potential) density surfaces. When the geostrophic divergence is expressed in terms of the vertical thickness, $h'$, of a parcel element, the two equations can then be integrated to give, respectively

$$f/h' = C_1 \tag{15}$$

and

$$-(\partial V_g/\partial n)/h' = C_2 \tag{16}$$

where the $C$'s are integration constants. Eq. (15) is often taken as representing the potential vorticity of all parcel elements in all geostrophic flows. In fact, eq. (15) is limited to two cases: the restricted one where individual parcels are in the geostrophic speed axis and the anomalous one where all parcels are without lateral shear and hence a geostrophic current of infinite lateral extent. The latter is sometimes applied to an idealized ocean interior.

In general, the constant $C_2$ in eq. (16) is not zero. For geostrophic anticyclonic shear is limited only by the inertial stability of the flow, according to Bjerkness (1951), while geostrophic cyclonic shear can be larger than $f$. Thus as long as the flow is stable, eq. (16) states that the lateral shear of a parcel in geostrophic motion can not change sign; that is, there can be no crossing of the speed axis. Hence eqs. (15) and (16) may be combined. One combination is

$$(f - \partial V_g/\partial n)/h' = C_3 \tag{17}$$

which is the law of conservation of geostrophic potential vorticity. The lateral shear in (17) is somewhat different from the lateral shear that Schmitz used in his potential vorticity equation, but the form of his equation is exactly that of (17). Hence the artifact that Schmitz introduced into his model is the constraint of geostrophic balance on cross-stream movement.

## Discussion and conclusion

The lateral shear vorticity is the negative of the lateral shear. Hence where the curvature and the lateral shear have the same sign, the corresponding vorticities have opposite signs. But this tendency to offset does not mean that the resulting relative vorticity may be taken constant or zero. In a three-dimensional flow, where horizontal divergence does not vanish, the relative vorticity of a meandering parcel must necessarily change, according to eqs. (8) and (11).

In a sluggish current, whether meandering or not, the relative vorticity is small because both the curvature and the shear vorticities are individually small. But in a fast, meandering current where curvature vorticity is large, the relative vorticity can remain small only when lateral shear vorticity of the opposite sign is present. Thus the contribution of the banking mechanism to the turning process has a twofold effect: a turning of the current and a concurrent damping of the amplitude of the resulting relative vorticity change. A parcel entering the left flank from the speed axis on approaching an anticyclonic turn gains positive (cyclonic) shear vorticity that offsets part of negative curvature vorticity gained in turning. Likewise, a parcel entering the right flank from the speed axis on approaching a cyclonic turn gains negative (anticyclonic) shear vorticity that offsets part of the positive curvature vorticity gained in turning. Hence, in crossing the speed axis, a meandering parcel is engaging in the process of keeping the magnitude of its relative vorticity change small.

In damping the amplitude of relative vorticity change, the banking mechanism acts through vertical motion and hence through individual change in horizontal speed. Therefore the amplitude of speed changes is generally larger than the amplitude of relative vorticity changes. Accordingly, the field of relative vorticity is generally a poor indicator of the intensity of the concurrent field of acceleration or of kinetic energy change. In particular, kinetic energy change will be underestimated in a model using geostrophic relative vorticity (Holton, 1972).

In a diagnostic study of a motion system, it is desirable to exhibit all the important mechanisms at work. In this sense, the choice of potential vorticity conservation is poor because it represents the net, integrated effect of different mechanisms. It is, of course, useful to know the net effect, but of even more importance to understanding the dynamics of the ocean is to know what are the different mechanisms and how they interact to achieve the net effect. For only such knowledge will lead to accurate prediction. In this context, it is also desirable to exhibit the mechanisms in terms of deterministic laws rather than in terms of statistical probability. In the framework of Reynolds equation of motion, an instantaneous motion field is replaced by the sum of a mean and a fluctuation field. What is not resolved by the mean field is automatically relegated to the fluctuation field whose representation is usually in terms of Reynolds stresses. By nature, these stresses are statistical, depending on correlations of flow components. Hence to the extent that the interaction process is represented by Reynolds stresses, the deterministic law governing the process is replaced by a statistical probability. But deterministic laws are more informative than statistical probabilities. Moreover, such processes as the interaction between curvature and lateral shear vorticities can be significant contributors to Reynolds stresses. Therefore, it is important in the study of interaction processes that we go beyond the routine computation of Reynolds stresses to find the governing deterministic laws, as was attempted here in the case of the interaction between curvature and lateral shear vorticities.

## Acknowledgements

I would like to thank Drs D. V. Hansen, A. Leetmaa, H. Mofjeld, and R. L. Molinari for reading the manuscript.

## REFERENCES

Bjerknes, J. 1951. Extratropical cyclones. In *Compendium of Meteorology*, American Meteor. Soc., Boston, pp. 1334.

Brown, D. 1959. *Diagram on drag forces on components of parachute drogues*. Scripps Institution of Oceanography, La Jolla, Calif.

Chew, F. 1974. The turning process in a meandering current, a case study. *J. Physical Oceanography 4*, 27–57.

Chew, F. & Berberian, G. A. 1972. Neighbor diffusivity as related to lateral shear in the Florida Current. *Deep Sea Res. 19*, 493–506.

Holton, J. R. 1972. *An introduction to dynamic meteorology*. Academic Press, New York, pp. 319.

Schmitz, W. J., Jr. 1969. On the dynamics of the Florida Current. *J. Marine Research 27*, 121–150.

## ВЗАИМОДЕЙСТВИЕ МЕЖДУ КРИВИЗНОЙ И БОКОВЫМ СДВИГОМ ВО ФЛОРИДСКОМ ТЕЧЕНИИ ПРИ СРЕДНЕМ И МГНОВЕННОМ СОСТОЯНИЯХ. СРАВНЕНИЕ

Путем сравнения двух случаев, относящихся к Флоридскому течению, рассматривается вопрос о том, насколько динамика мгновенного течения сохраняется в модели, выводимой из среднего состояния. В средней модели элементы жидкости не могут пересекать ось скорости. Однако наблюдения мгновенной картины течения обнаруживают взаимодействие вихрей, связанных с кривизной и боковым сдвигом, которое сопровождается систематическим перемещением элементов жидкости через ось скорости. Эта разница рассматривается с двух точек зрения. В начале рассматриваются уравнения, управляющие процессом взаимодействия, в частности, механизм превращения завихренности, связанной с кривизной, в завихренность, связанную с боковым сдвигом скорости и наоборот. Далее рассматривается динамика геострофического потенциального вихря. Делается вывод, что из-за геострофического приближения средняя модель не воспроизводит процесс взаимодействия.